The spin dependence of photoemission intensities off the surface normal, from the (1,1,1) face of platinum

1990 J. Phys.: Condens. Matter 2 5233

(http://iopscience.iop.org/0953-8984/2/23/014)

J. Phys.: Condens. Matter 2 (1990) 5233–5244. Printed in the UK

The spin dependence of photoemission intensities off the surface normal, from the (1,1,1) face of platinum

B Ginatempo† and B L Gyorffy‡

† Istituto di Fisica Teorica, Facolta' di Scienze, Universita' di Messina, Casella Postale 50, 1-98166 Villa Sant' Agata, Messina, Italy

‡ H H Wills Physics Laboratory, University of Bristol, Tyndall Avenue, Bristol BS8 1TL, UK

Received 22 February 1990

Abstract. Using a previously developed, relativistic theory of photoemission we calculate the off-normal photocurrent emerging from the (1,1,1) face of a platinum single crystal irradiated by normally incident, circularly polarised photons. We study the dependence of the photoemission intensities on the helicity of the photons and the spin and direction of the emitted electrons. Our results support the recent suggestion of Oepen and co-workers that photoemission experiments with circularly polarised light can provide useful information about the spin structure of the electronic spectra of solids, even if the spin polarisation of the photocurrent is not measured.

1. Introduction

Recently it has been suggested by Oepen *et al* (1986) that one can dispense with the expensive spin-polarisation analysis of photoemitted electrons and still learn something about the spin-dependent features of the band structure of solids if the incident photons are circularly polarised. In this paper we report a number of photocurrent calculations directly relevant to the experimental configurations employed by Oepen *et al* (1986) and later by Garbe and Kirschner (1989b) in their investigation of the Pt (1,1,1) face by photoemission spectroscopy using circularly polarised radiation. We will show that first-principles, more or less parameter-free calculations reproduce most features of the experimental data and provide strong support for the arguments put forward in the quoted papers.

In short we study photoelectrons, induced by circularly polarised radiation incident along the surface normal, emitted in off-normal directions. The physical effect of interest is the following. Due to spin–orbit coupling circularly polarised photons give rise to spin-polarised photoelectrons (Eyers *et al* 1984). Moreover when the helicity of the incident photons is reversed the spin orientation of the excited electrons changes sign. The interesting observation of Oepen *et al* (1986) was that the transmission of electrons through the surface also depends on their spin orientations. This effect is another consequence of the spin–orbit coupling. Furthermore, they have argued that as a result of this differential transmission of electrons with opposite spin orientation the spin-integrated photocurrent intensities will be different for left-handed (helicity+) and right-hanced (helicity−) incident radiation. This is, indeed, what they found.

0953-8984/90/235233 + 12 $03.50

A quantitative measure of the above effect is the intensity asymmetry A which was defined by Oepen *et al* (1986) as

$$A = (I^+ - I^-)/(I^+ + I^-) \tag{1}$$

where $I^\pm$ are the measured photocurrent intensities for incident photons with $\pm$ helicity. They studied A as a function of the kinetic energy of the outgoing electrons. Recently, Garbe and Kirschner (1989b) published a more extensive investigation of A. Our aim here is to comment on their findings in the light of first-principles calculations of the photocurrent. Our results fully support their semi-phenomenological analysis and interpretation of the experimental data.

Of course, the calculation of the total photocurrents, $I^\pm$, proceeds through the calculation of their spin components, $I^\pm_{\text{up}}$ and $I^\pm_{\text{down}}$ via the relation $I^\pm = I^\pm_{\text{up}} + I^\pm_{\text{down}}$. Although in experiments using Mott detectors for collecting the photoemitted electrons $I^\pm_{\text{up}}$ and $I^\pm_{\text{down}}$ are measured directly (Garbe and Kirschner 1989a), in the experiments of interest here only $I^\pm$ is recorded. Nevertheless, it will be seen that the knowledge of the spin components $I^\pm_{\text{up}}$ and $I^\pm_{\text{down}}$ can be extremely useful in the analysis of the measured intensity asymmetries.

Our calculations are based on a fully relativistic theory of the photoemission process and hence automatically include a full description of the spin–orbit coupling, which is the root cause of the intensity asymmetry. The theory was developed by Ginatempo *et al* (1985) and a detailed account of it has been given in a recent publication (Ginatempo *et al* 1989). Nevertheless, in the interests of clarity, we shall briefly review its main features in section 2.

An alternative but closely related theory was developed by Ackermann and Feder (1985). The extent to which our calculations agree with those based on that will be illustrated in section 2.

In section 3 we compare our results with the experiments and in section 4 we comment on the interpretation of their data by Garbe and Kirschner. We summarise our conclusions in section 5.

2. On the formal aspects of the theory

In this section we recall, briefly, some of the principal features of the formal theory (Ginatempo *et al* 1985, 1989). We study the probability of electrons being photoemitted in the direction $\hat{\boldsymbol{n}}_e$, defined by the angles θ_e. φ_e, as a consequence of photons incident along the surface normal with helicity ± 1. The geometrical arrangement of the various directions in the problem is depicted in figure 1. All through this paper the surface through which the photoelectrons pass is the (1,1,1) surface of an FCC Pt crystal and the various potential functions are designed to reflect this fact quantitatively. In fact they have been extracted from a relativistic self-consistent LMTO calculation of the band structure which gave results virtually equivalent to those of Guo and Temmerman (1989).

Although it is often useful to analyse photoemission experiments in terms of transitions between bulk states, propagation to the surface and refraction at the surface, a fully consistent theory of the photoemission process recognises that real electrons make transitions between the states of the semi-infinite solid with a surface in a single step. Our theory describes this one-step process following the multiple-scattering approach of Pendry (1976).

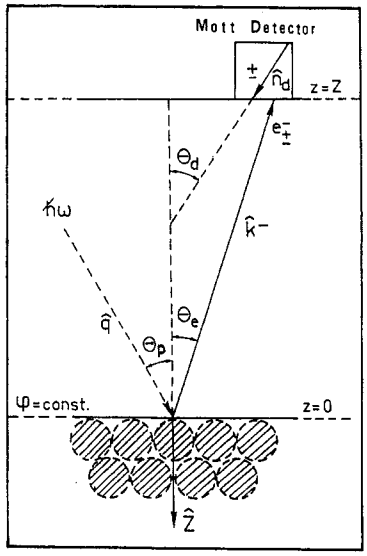

Figure 1. The directions and angles relevant to a calculation of spin-polarised photoemission intensities.

The logic of the theory is the opposite to the physical process. We start by defining the state of the final electron at the Mott detector by the relativistic plane wave:

$$\langle r|f,\lambda\rangle = \sum_{G} q_\lambda^s U_\lambda^s(\varepsilon+\hbar\omega, k_\parallel r)\exp(-ik_\parallel r)\delta(z-Z) \tag{2}$$

where λ stands for 'up' and 'down' and refers to the spin direction accepted by the Mott detector with an internal axis of spin quantisation along $\hat{\boldsymbol{n}}_d \equiv (\theta_d, \varphi_d)$, U_λ^s is the usual four-spinor amplitude of the plane wave with $s = \pm 1$ denoting the spin state of the photoelectron with respect to the surface normal, and the coefficients q_λ^s are defined by

$$\begin{aligned} q_{up}^{+} &= \cos(\theta_d/2) & q_{up}^{-} &= \exp(i\theta_d)\sin(\theta_d/2) \\ q_{down}^{+} &= -\exp(-i\varphi_d)\sin(\theta_d/2) & q_{down}^{-} &= \cos(\theta_d/2). \end{aligned} \tag{3}$$

Having defined the final state at the detector it is then matched to the time-reversed LEED states in the bulk. Finally, the amplitudes of such states are calculated by regarding them as having been induced by a circularly polarised photon incident along the surface normal with helicity $\nu = \pm 1$. Thus for a given photon energy $\hbar\omega$, emission direction $\hat{\boldsymbol{n}}_e$ and Mott detector orientation $\hat{\boldsymbol{n}}_d$ we calculate four spectra

$$I_{up}^{\nu=+}(\varepsilon,\omega,\hat{\boldsymbol{n}}_e,\hat{\boldsymbol{n}}_d) \quad I_{down}^{\nu=+}(\varepsilon,\omega,\hat{\boldsymbol{n}}_e,\hat{\boldsymbol{n}}_d) \quad I_{up}^{\nu=-}(\varepsilon,\omega,\hat{\boldsymbol{n}}_e,\hat{\boldsymbol{n}}_d) \quad I_{down}^{\nu=-}(\varepsilon,\omega,\hat{\boldsymbol{n}}_e,\hat{\boldsymbol{n}}_d).$$

From these we construct the intensities

$$I^{+} = I_{up}^{\nu=+} + I_{down}^{\nu=+} \qquad I^{-} = I_{up}^{\nu=-} + I_{down}^{\nu=-}. \tag{4}$$

These are the intensities that are measured when no Mott detector is used. That is to say when both up and down electrons are accepted by the detector. Namely, these are the intensities measured by the experiments of interest here.

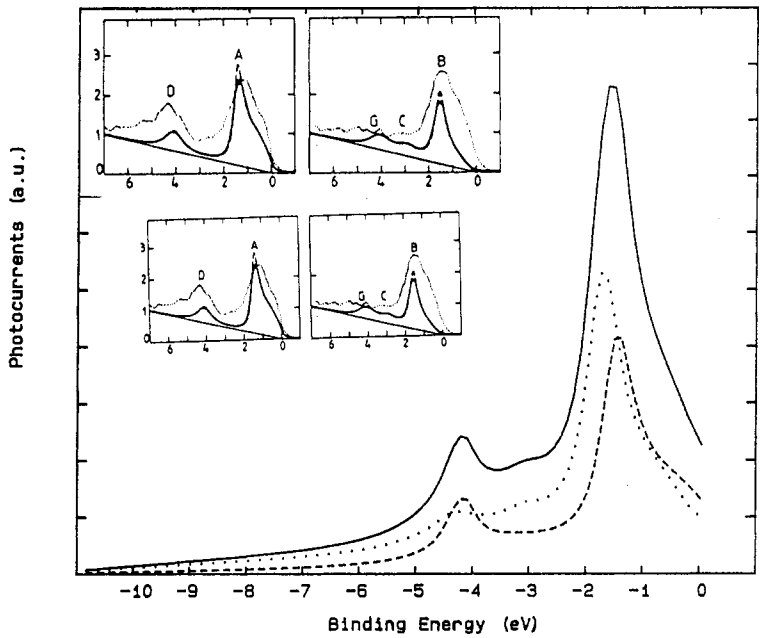

Figure 2. Calculated spin-resolved photocurrents for the case of normal incidence and normal emission from the (1,1,1) face of Pt, for a photon energy of $\hbar\omega = 25$ eV and right circular polarisation. Full curve: total intensity; broken curve: up intensity; dotted curve: down intensity. The inset shows the analogous calculation of Tamura *et al* (1989) for the up (on the left) and down (on the right) photocurrents and the experimental results of Garbe and Kirschner (1989b).

Following Oepen *et al* (1986) we shall focus much attention on the intensity anisotropy defined by (1). We shall also find it useful to study the polarisation of the photocurrent given by

$$\mathcal{P} = \mathcal{P} \cdot \hat{\boldsymbol{n}}_a = (I^{\nu}_{\uparrow} - I^{\nu}_{\downarrow})/(I^{\nu}_{\uparrow} + I^{\nu}_{\downarrow}). \tag{5}$$

Having decided on the crystal surface to study, the corresponding potential functions and the experimental geometry, in the above theory there are two more choices to be made. These are the description of the surface potential barrier and the mean free path of the excited electrons travelling towards the surface. The physical origins of both of these quantities are subtle and deserve separate theories in their own rights (see, for example, Feder (1985) and references therein). However, in this, first-pass, attempt to study the phenomenon at hand we have contented ourselves with the simplest recipes of each case. For the former we used a simple step function of height 0.9 Ryd and for the latter we used two energy-independent optical potentials (inverse lifetimes): $A = \mathcal{A} \cdot \mathcal{P} = V_{0i} = -20$ m Ryd and $V_{pi} = -300$ m Ryd respectively for the low- and high-energy states.

For general orientation we display in figure 2 the spin components of a photoelectron spectrum corresponding to normal incident normal emission from a Pt (1,1,1) surface as calculated by following the procedure described above. The incident photon energy was taken to be $\hbar\omega = 25$ eV. In the inset we display the results of the corresponding calculations by Tamura *et al* (1989) together with the experimental spectra of Garbe and

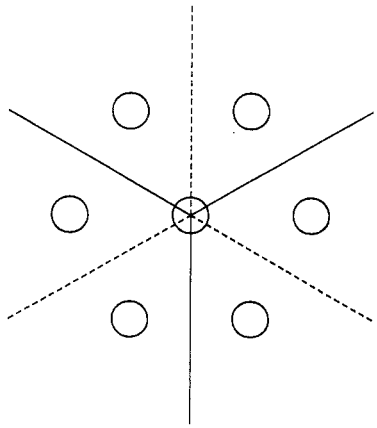

Figure 3. The C_{3v} symmetry of the FCC (1,1,1) surface. Circles represent atoms. Straight lines represent the intersections of the three ΓLUX mirror planes with the surface. Full and broken portions of the intersections represent the non-equivalent sides of the mirror planes with respect to the threefold symmetry axis.

Kirschner (1989a). The first point we wish to make is that although the two calculations differ in many practical details the results are in good quantitative agreement. This suggests that in spite of their complexity these large fully relativistic one-step-process calculations can be reliably implemented.

Our second point refers not to the above comparison between two calculations but to their relevance to experiments. We note that Tamura *et al* (1989) studied normal-emission spectra from the Pt (1,1,1) face in considerable detail and found satisfactory agreement with the experiments of Garbe and Kirschner (1989a). This establishes our calculational scheme as a credible method for studying the intensity asymmetries for off-normal emission on this particular surface.

Finally we stress that using non-relativistic instead of relativistic quantum mechanics to calculate the intensity asymmetry A would yield zero. This is in agreement with the symmetry arguments of Oepen *et al* (1986), according to which $A \neq 0$ is a consequence of spin–orbit coupling. We also checked the selection rule according to which the intensity anisotropy is zero along mirror planes. For later reference we show in figure 3 the intersections of the three mirror planes of the (1,1,1)-face, with C_{3v} symmetry, and the (1,1,1) surface. Although $A = 0$ along these lines the photocurrent is not the same along the full portions of the lines as along the broken portions. However, the intensities are the same along the three full lines and also along the three broken lines as required by the threefold axis of symmetry perpendicular to the (1,1,1) surface of an FCC lattice.

3. The calculated photocurrents

With the purpose of interpreting the data of Garbe and Kirschner (1989b), we have performed the calculations of the photoemission spectra corresponding to a photon beam of energy $\hbar\omega = 18$ eV incident along the surface normal of either right or left circular polarisation. The emission angle is fixed as $\theta_e = 62°$. In all the calculations the number of beams for the plane-wave expansion of the multiple-scattering matrices is fixed as 19, which corresponds to the first 4 shells of the (1,1,1)-layer reciprocal vectors. The corresponding results for several values of the azimuth angle $\varphi_e = \varphi_q = \varphi$ ($\varphi = 0$ corresponds to the emission direction lying in the ΓLUX mirror plane) are shown in

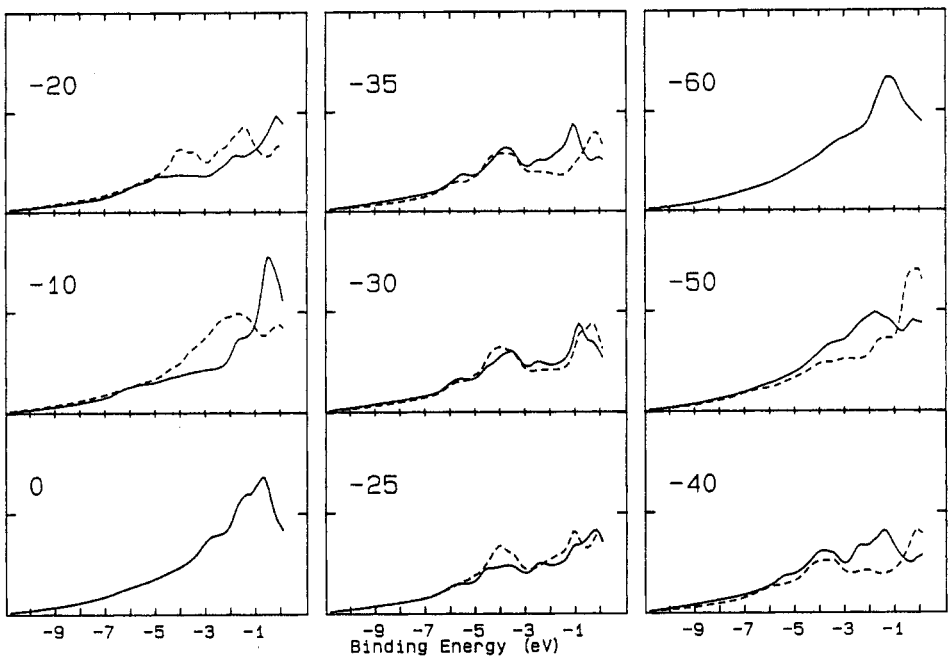

Figure 4. The calculated photocurrents versus the azimuth angle φ. Positive- and negative-helicity photons are incident normally onto the (1,1,1) surface of Pt; $\hbar\omega = 18$ eV; $\theta_e = 62°$. Full curves correspond to positive helicity, broken curves to negative helicity. The number in the upper left corner of each panel indicates the value of φ.

figure 4, where the full and broken curves refer to the spectra calculated for radiation of positive and negative helicity respectively.

The first thing to note about these results is that no asymmetry has been found for $\varphi = -0°$ and $\varphi = -60°$ (i.e. two mirror planes). Moreover, these spectra look different. Evidently, both these facts are in agreement with the symmetry analysis of the preceding section. Note also that in figure 4 only the calculations for negative φ are displayed. The spectra corresponding to positive values of φ are identical to those for negative ones, with the difference that the helicities are interchanged. This symmetry was predicted and to some extent observed by Garbe and Kirschner (1989a). The experimental violations of it can be easily explained by misalignment of the sample.

An unexpected feature of our calculation is the almost symmetric interchange between I^+ and I^- across the $\varphi = 30°$ line. Clearly this interchange corresponds to a change of sign of the asymmetry A. The extent to which A at -10, -15, -20 and -25 is equal to $-A$ at -50, -45, -40 and -35 is displayed in figure 5. Reassuringly the experiment data by Garbe and Kirschner (1989a) also manifest the above phenomena. A quantitative comparison between the corresponding theory and the experiment will be given in the next section, together with an explanation of it.

A rough comparison between theory and experiment shows a gratifying agreement over the positions of the larger peaks and even the relative amplitudes are often right. However, there are many more small bumps in the theoretical curves than can be identified in the experimental data. These may be due to bands in the wrong places in energy or to inadequate treatment of the lifetime effect. In connection with the latter

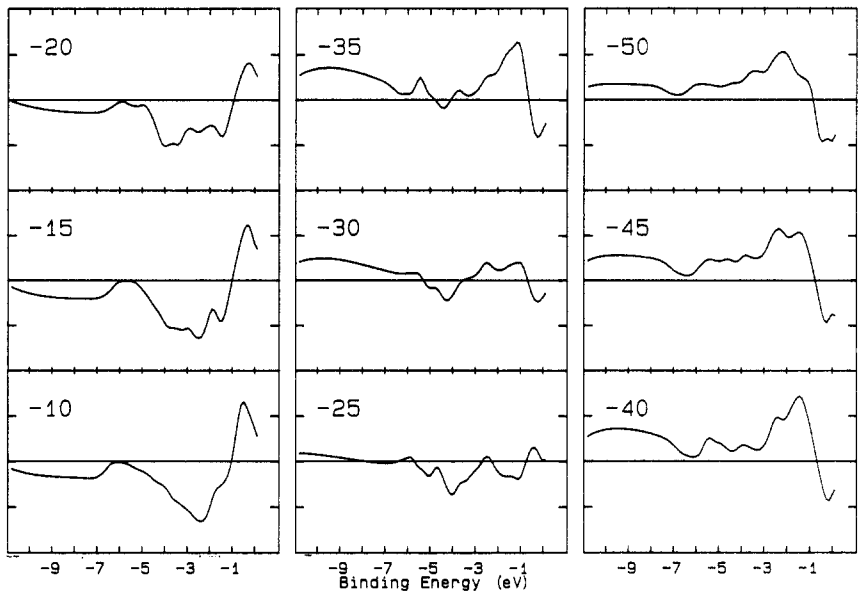

Figure 5. The calculated asymmetry spectra versus the azimuth angle φ. The number in the upper left corner of each panel indicates the value of φ.

we would like to stress, again, that we could improve the quantitative agreement between theory and experiment substantially by using energy-dependent lifetimes which shorten for higher binding energy. This should smooth out many of the small structures in the calculation below -4 eV where the experiment is quite structureless. Nevertheless, as we have mentioned in the introduction, we did not do this. To illustrate the effect of the assumed lifetime on the appearance of the calculated spectra we display in figure 6 the photocurrents for $\hbar\omega = 12$ eV, $\hat{\boldsymbol{n}}_e = (44°, 12.75°)$, $\hat{\boldsymbol{n}}_d = (0°, 12.75°)$ calculated with inverse lifetimes $V_{0i} = -20$ mRyd (left-hand panel) and $V_{0i} = -10$ mRyd (right-hand panel). Evidently halving the lifetime makes a number of small features disappear.

4. Analysis of the results

To investigate quantitatively the changes in A on crossing the $\varphi = 30°$ emission direction we wish to focus attention on the dominant peak at -1.5 eV which has been identified by Garbe and Kirschner (1989b) as due to the emission from band 4, according to the labelling of the bands by Oepen. We have calculated the asymmetry A for various values of φ and the results are displayed in figure 7 together with the experimental points. Clearly, the agreement in the range $-30 < \varphi < 30$ is excellent and lends strong support to the conclusion that the theory does in fact describe what has been observed in the experiment. The fact that the agreement is getting poorer as the angular distance from $\varphi = 0$ increases supports the explanation that it is due to a misalignment of the sample.

Another useful way of making contact with the experimental observation is to calculate the polarisation of the emerging photocurrent. Garbe and Kirschner (1989b) argued that the contributions to this quantity from band 4 and 5 should be roughly

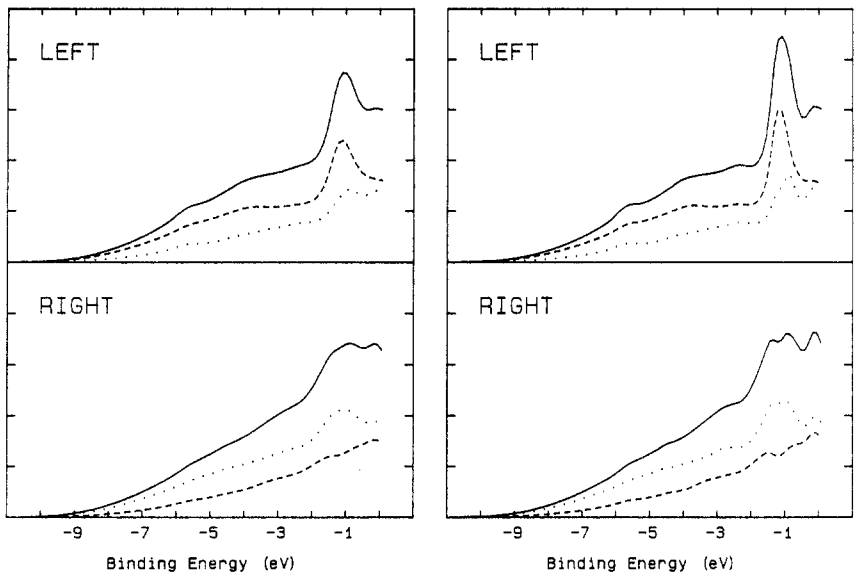

Figure 6. The total photoelectron spectra and their *up* and *down* components from Pt (1,1,1) excited by normally incident photons of left and right circularly polarised radiation of energy $\hbar\omega = 12$ along $\hat{n}_e = (44°, 12.75°)$ and detector quantisation axis $\hat{n}_d = (0°, 12.75°)$. The left-hand panels refer to a calculation performed with V_{0i} = -20 mRyd, the right panels to V_{0i} = −10 mRyd. The light polarisation is as indicated.

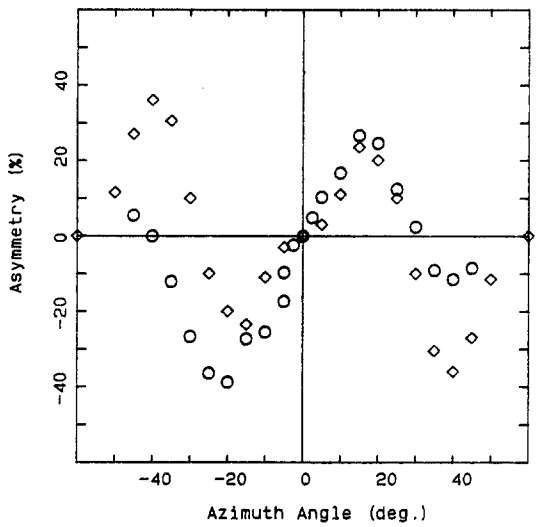

Figure 7. The asymmetry of band 4 versus the aximuth angle φ. Open circles: experimental data of Garbe and Kirschner (1989a); rhombohedra: theoretical prediction.

perpendicular (see also same paper as before). We calculate for $\varphi = 0°$ the up and down component of the photocurrent with respect to a detector z axis which is at first in the longitudinal ($\hat{n}_d = 0°, 0°$)) and then in the transverse ($\hat{n}_d = (90°, 90°)$) direction. They

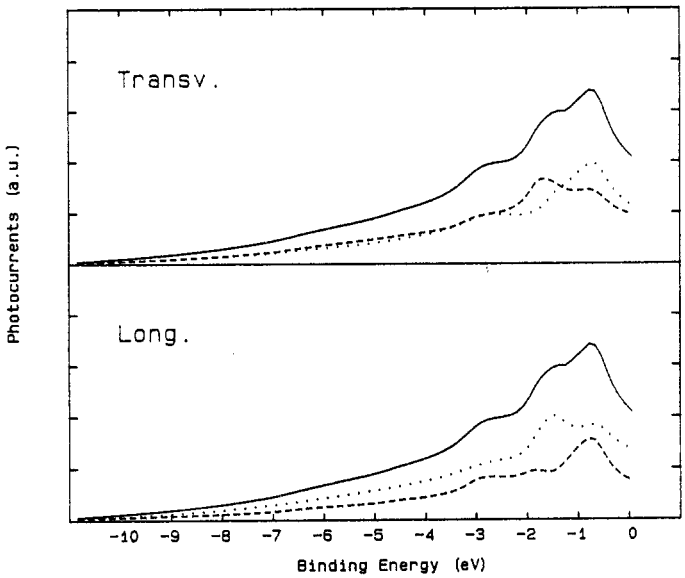

Figure 8. The total and spin components of the photoelectron spectra for the longitudinal, $\hat{\boldsymbol{n}}_d = (0°, 0°)$, and transverse, $\hat{\boldsymbol{n}}_d = (90°, 90°)$, orientation of the Mott detector, with respect to the mirror plane. The photon energy is $\hbar\omega = 18$ eV; the polarisation is right circular; the emission direction is $\hat{\boldsymbol{n}}_e = (62°, 0°)$. Full curves: total photocurrent; broken curves: *up* photocurrents; dotted curves: *down* photocurrents.

are shown in figure 8. Note that the two peaks at binding energies $\simeq 0.75$ eV and -1.75 eV correspond to bands 4 and 5 respectively. Evidently, the total photocurrents for the two different orientations of the detector are the same. Next we evaluate the spin polarisation as defined in (5), along the two z axes. The results of these calculations are shown in figure 9. The various features for binding energies above -2 eV are, again, due to bands 4 and 5. Clearly, with respect to their signs the two peaks behave in opposite manners. From these components of the polarisation we can reconstruct the full polarisation vector at every energy. For energies corresponding to the approximate positions of the band-4 and band-5 peaks we show the component parallel and orthogonal to the mirror plane of polarisation vectors $\mathcal{P}_4$ and $\mathcal{P}_6$ in figure 10. Full and broken vectors refer to the uncertainty related to the finite width of the corresponding peak in figure 9. Thus the deductions of Garbe and Kirschner (1989b) that $\mathcal{P}_4$ is roughly perpendicular to $\mathcal{P}_6$ is born out by our detailed calculation.

Finally, we wish to comment on the origin of the approximate symmetry of the anisotropy A across the $\varphi = 30°$ plane of the emission direction. Clearly, if $A(30° - \delta; \varepsilon) = -A(30° + \delta; \varepsilon)$ was directly true for each energy ε the surface would appear to have the sixfold rotational symmetry about the surface normal instead of the actual, threefold, symmetry of the (1,1,1) face of an FCC lattice. Note, however, that the top layer of atoms have precisely the sixfold axis of symmetry mentioned above, In fact each layer on its own has this symmetry but the spacing of the subsequent layers breaks it by rotating the layers through 30° and $-30°$ alternatively with respect to each other. Our suggestion is that the photoemission intensity is dominated by the contribution from the top layer and fails to have the full hexagonal symmetry only because the contributions from the other layers is not negligible. In support of the above hypothesis we can

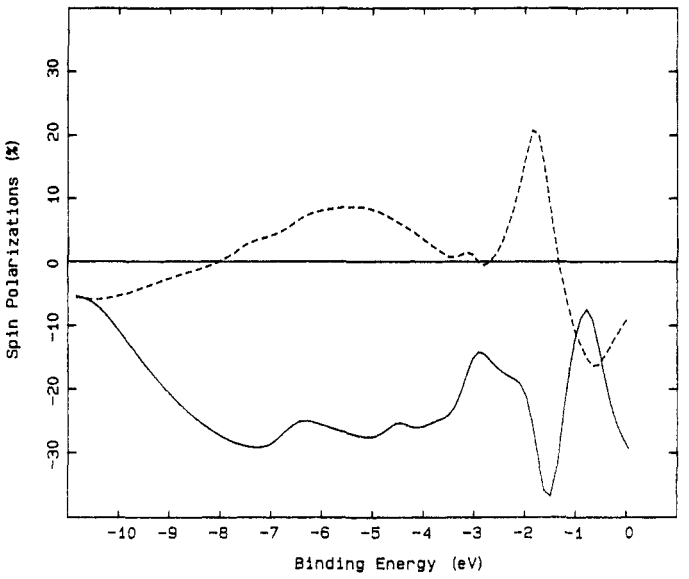

Figure 9. The spin polarisations relative to the calculation of figure 7. Full curve: longitudinal components; broken curve: transverse component.

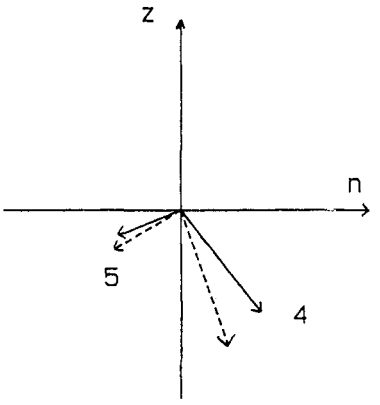

Figure 10. The polarisation vectors of photoelectrons originating from the bands 4 and 5 at $\varphi = 0°$, as deduced from the spin-polarisation spectra of figure 8. $\hat{z}$ is the surface normal; $\hat{n}$ is a unit vector lying on the surface and orthogonal to the mirror plane. The full and broken vectors represent the possible variation of the polarisation vectors due to the finite width of the corresponding peaks in the spin polarisation (see the text).

offer the following argument. The relative contributions from the various layers to the photocurrent are greatly influenced by the lifetime. The scattering described by the inverse lifetime gives rise to a short mean free path for the outgoing electrons and will increase the relative importance of the contribution from the top layer at the expense of those coming deeper down in the sample. Thus, if our hypothesis is correct, reducing the inverse lifetime should mean that $A(30°; \varepsilon)$ gets smaller less rapidly than $A(20°; \varepsilon)$ or $A(40°; \varepsilon)$. As shown in figure 11 this is indeed what we find. Consequently, the approximate *hexagonal symmetry* of the observed anisotropy is due to the influence of the top layer and hence a dramatic measure of the surface sensitivity of this particular probe.

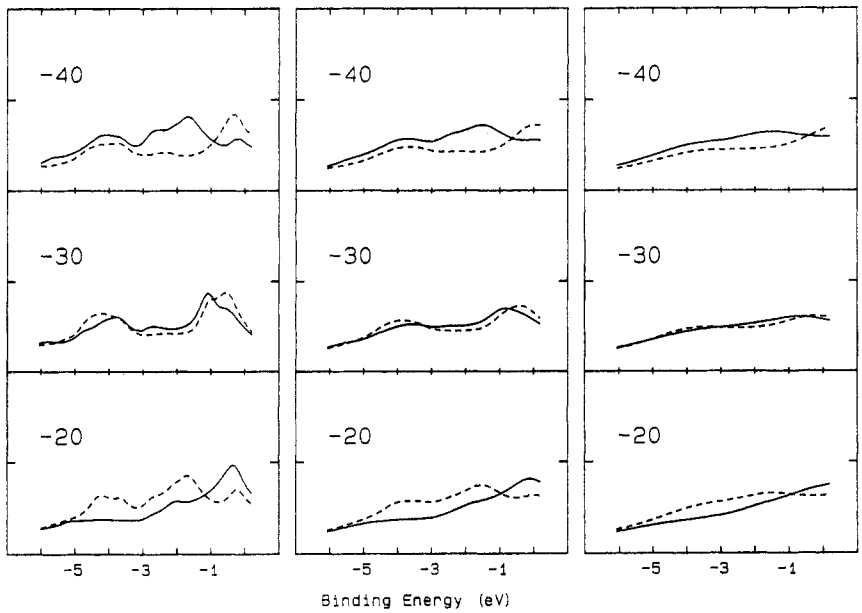

Figure 11. The photoemission spectra and their asymmetry versus the inverse lifetime V_{0i}. Left-hand panel: the spectra for $\hbar\omega = 18$ eV, positive and negative helicity, $\theta_e = 62°$, the indicated azimuth angles φ (−20, −30, −40) and $V_{0i} = -20$ mRyd. Middle panel: the same as the left-hand panel but for $V_{0i} = -40$ mRyd. Right-hand panel: the same as the left-hand panel but for $V_{0i} = -80$ mRyd. Full curves: positive helicity; broken curves: negative helicity.

5. Conclusion

We have studied the photoemission intensity asymmetry $A(\hat{n}_e; \varepsilon)$ discovered by Oepen *et al* (1986). In off-normal photoemission from the Pt (1,1,1) face for circularly polarised, normally incident photons. We found that a fully relativistic, first-principles calculation, which gives an adequate account of the photoelectric spectra, reproduces the most dominant features of $A(\hat{n}_e; \varepsilon)$. Moreover, our calculations support the interpretation of the relevant experimental data by Oepen *et al* (1986) and Garbe and Kirschner (1989b). In short, we provided further evidence that the photoemission intensity asymmetry (PIA) can be a useful probe of the spin-dependent features of the electronic structure. Moreover, we called attention to the extreme surface sensitivity of the effect.

Evidently, in addition to providing information about the spin structure of the electronic states, the above effect might also be useful in detecting the helicity of incident photons in the UV range. The surprisingly large value of A found for Pt (1,1,1) suggests that this metal surface is a good candidate for such a use.

Acknowledgments

We would like to thank Professor J Kirschner for a very useful conversation and Drs W M Temmerman and C Y Guo for having provided the potential used in this calculation and the relative band structure. One of us (BG) acknowledges the contribution of CNR,

Italy, for supplying CRAY-XMP resources at CINECA (Bologna, Italy) where some of the calculations presented were performed.

References

Ackermann A and Feder R 1985 *J. Phys. C: Solid State Phys.* **18** 1093
Eyers A, Schäfers F, Schönhense G, Henzmann U, Oepen H P, Hünlich K, Kirschner J and Borstel G 1984 *Phys. Rev. Lett.* **52** 1559
Feder R 1985 *Polarized Electrons in Surface Physics* ed R Feder (Singapore: World Scientific) p 125
Garbe J and Kirschner J 1989a *Phys. Rev.* B **39** 1530
—— 1989b *Phys. Rev.* B **39** 9859
Ginatempo B, Durham P J and Gyorffy B L 1989 *J. Phys.: Condens. Matter* **1** 6483
Ginatempo B, Durham P J, Gyorffy B L and Temmermann W M 1985 *Phys. Rev. Lett.* **58** 1581
Guo C Y and Temmerman W M 1989 private communication
Oepen H P, Hünlich K and Kirschner J 1986 *Phys. Rev. Lett.* **56** 496
Pendry J B 1976 *Surf. Sci.* **57** 679
Tamura E, Piepke W and Feder R 1989 *J. Phys.: Condens. Matter* **1** 6469